

On the X-ray efficiency of the white dwarf pulsar candidate ZTF J190132.9+145808.7

Aya BAMBA^{1,2,3}, Yukikatsu TERADA⁴, Kazumi KASHIYAMA^{5,6}, Shota KISAKA⁷, Takahiro MINAMI^{1,6} and Tadayuki TAKAHASHI^{6,1}

¹Department of Physics, Graduate School of Science, The University of Tokyo, 7-3-1 Hongo, Bunkyo-ku, Tokyo 113-0033, Japan

²Research Center for the Early Universe, School of Science, The University of Tokyo, 7-3-1 Hongo, Bunkyo-ku, Tokyo 113-0033, Japan

³Trans-Scale Quantum Science Institute, The University of Tokyo, Tokyo 113-0033, Japan

⁴Graduate School of Science and Engineering, Saitama University, 255 Shimo-Ohkubo, Sakura, Saitama 338-8570, Japan

⁵Astronomical Institute, Tohoku University, Sendai 980-8578, Japan

⁶Kavli Institute for the Physics and Mathematics of the Universe, The University of Tokyo, Kashiwa 277-8583, Japan

⁷Physics Program, Graduate School of Advanced Science and Engineering, Hiroshima University, Higashi-Hiroshima 739-8526, Japan

*E-mail: bamba@phys.s.u-tokyo.ac.jp

Received ; Accepted

Abstract

Strongly magnetized, rapidly rotating massive white dwarfs (WDs) emerge as potential outcomes of double degenerate mergers. These WDs can act as sources of non-thermal emission and cosmic rays, gathering attention as WD pulsars. In this context, we studied the X-ray emissions from ZTF J190132.9+145808.7 (hereafter ZTF J1901+14), a notable massive isolated WD in the Galaxy, using the Chandra X-ray observatory. Our results showed 3.5σ level evidence of X-ray signals, although it is marginal. Under the assumption of a photon index of 2, we derived its intrinsic flux to be $2.3 (0.9\text{--}4.7) \times 10^{-15} \text{ erg cm}^{-2}\text{s}^{-1}$ and luminosity $4.6 (2.0\text{--}9.5) \times 10^{26} \text{ erg s}^{-1}$ for a 0.5–7 keV band in the 90% confidence range, given its distance of 41 pc. We derived an X-ray efficiency (η) concerning the spin-down luminosity to be 0.012 (0.0022–0.074), a value comparable to that of ordinary neutron star pulsars. The inferred X-ray luminosity may be compatible with curvature radiation from sub-TeV electrons accelerated within open magnetic fields in the magnetosphere of ZTF J1901+14. Conducting more extensive X-ray observations is crucial to confirm whether ZTF J1901+14-like isolated WDs are also significant sources of X-rays and sub-TeV electron cosmic rays, similar to other WD pulsars in accreting systems.

Key words: white dwarfs — acceleration of particles — magnetic fields — X-rays: individual (ZTF J190132.9+145808.7) — equation of state

1 Introduction

Low-mass stars like our Sun evolve into white dwarfs (WDs) at the end of their lifetimes. One-third of stellar objects are believed to be white dwarfs. These objects are significant not only as major constituents of the Galaxy but also as key entities for understanding physics under high density environments, the mechanism of SN Ia explosions, and more. Additionally, WDs close to the Chandrasekhar limit are pivotal for the substantial production of neutronized species like ^{58}Ni and ^{55}Mn through efficient electron capture processes (Iwamoto et al. 1999; Seitenzahl et al. 2013).

Massive and rapidly rotating WDs are of particular interest because they can form through WD-WD mergers (Dan et al. 2014). As a result of such mergers, these massive WDs possess a smaller radius and higher density, consistent with their equation of states ($MR^{1/3} \approx \text{const.}$, where M and R denote mass and radius respectively; (Schwab 2021)). A more rapid rotation period is anticipated due to the conservation of angular momentum, although the extent of this conservation remains a topic of study (Schwab 2021). Their dipole magnetic fields are believed to be intensified by potent dynamo mechanisms during mergers (Tout et al. 2008; García-Berro et al. 2012; Das & Mukhopadhyay 2012).

Identifying and quantifying such massive and rapidly rotating WDs are crucial steps in understanding WD-WD merger rates and their associated nucleosynthesis processes. While massive WDs typically exhibit high-temperature colors in the optical band, most have spin periods around 10^4 s or longer. Recent deep optical surveys have identified several potential remnants of WD-WD mergers with rapid spin periods. One notable candidate identified by the Zwicky Transient Facility is ZTF J190132.9+145808.7 (hereafter ZTF J1901+14). This WD is near the Chandrasekhar limit with a mass between $1.327\text{--}1.365 M_{\odot}$, a measured radius comparable to the Moon, and a notably short spin period of 416 s (Caiazzo et al. 2021).

We propose an innovative approach to investigate these magnetic and rapidly rotating WDs. They are expected to emit nonthermal X-rays as a result of their spin-down, akin to isolated neutron stars, leading to their nickname “white dwarf pulsars”. Such WDs are anticipated to release hard pulsating X-rays, presenting a novel method for their identification. Ostriker et al. (1970) originally proposed this idea. Observationally, the first such X-ray emission was reported from an accreting magnetized WD, AE Aqr (Terada et al. 2008), which has an incredibly fast rotation period of 33 s. This was followed by discoveries in AR Sco (Buckley et al. 2017; Takata et al. 2018) with a period of 118 s and J191213.72–441045.1 (Pelisoli et al. 2023) with a period of 5.30 min. Their rapid spin, significant magnetic field, and larger radius compared to neutron stars enable them to achieve electrostatic potentials, $V \propto P^{-2}BR^{3/2}$, comparable to those of neutron stars. Consequently, WD pulsars can accelerate particles to as high energies as neutron stars. The X-ray luminosity from these WDs is around 0.1% of their spin-down energy (Terada et al. 2008), similar in efficiency to neutron stars (Kargaltsev & Pavlov 2008). Given the abundance of WDs compared to neutron stars, they might significantly contribute to the Galactic cosmic ray electron-positron components (Kashiyama et al. 2011; Kamae et al. 2018). Notably, some radio sources labeled “ultra-long period pulsars” could be white dwarfs, providing further evidence of white dwarf pulsars (Hurley-Walker et al. 2022; Hurley-Walker et al. 2023).

However, all identified WD pulsars to date are part of accreting systems. Earlier hard X-ray observations of isolated WDs failed to detect significant nonthermal emissions (Harayama et al. 2013), and the constraints from these observations were somewhat loose. A focused search for isolated WD pulsars is necessary to validate our proposed scenario. In this paper, we present the first nonthermal X-ray search for the massive, high-magnetic field WD, ZTF J1901+14, using the high-resolution capabilities of the Chandra observatory. In Section 2, we detail our target selection, observation methods, and data reduction. Section 3 outlines our imaging and spectral analysis results, while Section 4 offers a discussion of our findings.

2 Target Selection and observations

Our primary goal is to detect X-rays emitted from isolated, massive, and magnetic white dwarfs (WDs) that exhibit short spin periods. Recent optical surveys, such as the Zwicky Transient Facility (Bellm et al. 2019) and the Sloan Digital Sky Survey (Eisenstein et al. 2006), have identified several isolated WDs that rotate rapidly. Out of 25 WDs from Kilic et al. (2023), which catalogs ultramassive WDs, we singled out four as potential WD pulsar candidates, based on their strong magnetic fields and rapid rotation. Table 1 showcases the physical parameters of these candidates, juxtaposed with EUVE J0317–855, which has been previously investigated as a WD pulsar candidate (Harayama et al. 2013).

Dipole moments (μ) and spin-down energy (\dot{E}) were estimated, assuming the relationships $\mu \propto BR^3$ and $\dot{E} \propto \mu^2 P^{-4} \propto$

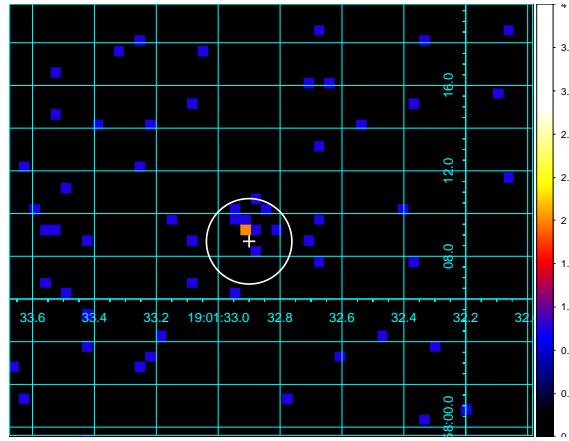
Table 1. Properties of WD pulsar candidates.

	ZTF J1901+14	J032900.79–212309.24*	J070753.00+561200.25*	J221141.80+113604.5*	EUVE J0317–855
Distance d (pc)	41	59	87	69	27
Mass (M_{\odot})	1.327–1.365	1.344	1.291	1.27	1.34±0.3
Radius R (km)	2140	2366 [†]	2978 [†]	3194 [†]	2417 [†]
Period P (s)	416	558	3780	70	725
Magnetic field B (MG)	600–900	50–100	no data	15	450
Dipole moment μ^{\ddagger}	0.93–1.39	0.10–0.21	no data	0.08	1
Spin-down energy \dot{E}^{\ddagger}	7.9–17.8	0.03–0.12	no data	68	1
Spin-down flux $\dot{E}/4\pi d^2$	3.4–7.7	0.006–0.02	no data	10.4	1
References	(1)	(2)	(2)	(3)	(4)(5)

* SDSS name.

[†] Estimated with the best-fit value and Nauenberg (1972).[‡] Normalized to \dot{E} of EUVE J0317–855.

Note — (1) Caiazzo et al. (2021), (2) Kilic et al. (2023), (3) Kilic et al. (2021), (4) Kawka et al. (2007), (5) Harayama et al. (2013)

**Fig. 1.** All-band count image of ZTF J1901+14 region. No vignetting correction has been applied. The scale is in linear, and the coordinates are in J2000. The white cross and circle represent the cataloged position of ZTF J1901+14 by SIMBAD and its error range with the radius of 2 arcsec.

$B^2 R^6 P^{-4}$, where R represents their radius and P is their rotation period. We utilized Nauenberg (1972) to determine R , as detailed in Table 1. It is worth noting that strong magnetic fields might induce minor variations in R , but for our approximate calculations, such effects are negligible. Table 1 also presents the derived \dot{E} , normalized by the value for EUVE J0317–855.

A crucial parameter for detecting significant X-ray emissions is the spin-down flux, denoted by $\dot{E}/(4\pi d^2)$, where d is the distance to the target (refer also to Shibata et al. (2016); Watanabe et al. (2019); Bamba et al. (2020)). As observed, ZTF J1901+14 and SDSS 221141.80+113604.5 are poised to exhibit the highest spin-down flux among the five WD pulsar candidates, making them ideal subjects for our investigation. However, only ZTF J1901+14 has undergone observations with X-ray observatories, leading us to choose it as our primary target.

ZTF J1901+14 was observed by Chandra ACIS-I (Weisskopf et al. 2002) on 2022/12/09–10 (OBSID: 26496, 27596, and 27597). The data reduction and analysis was done with CIAO 4.15 (Fruscione et al. 2006) and CALDB version of 4.10.4. We made the reprocessed cleaned data with the standard method following the CIAO guide, and the resultant exposure time is 39.3 ks.

3 Results

Figure 1 displays the 0.5–7 keV image of the ZTF J1901+14 region. In this figure, the position of our target, as determined by SIMBAD (Wenger et al. 2000), is marked with a white cross. Note that the pixel scale of the CCD onboard ZTF is 1 arcsec and the median delivered image quality is 2.0 arcsec in full width at half maximum¹.

¹ <https://www.ztf.caltech.edu/ztf-camera.html>

Table 2. Properties of WD pulsars and ZTF J1901+14.

	AE Aqr	AR Sco	J191213.72–441045.1	EUVE J0317–855	ZTF J1901+14
Type	accreting	accreting	accreting	isolated	isolated
Distance (pc)	92	117	237	27	41
P (s)	33	118	319	725	416
B (MG)	50	900	no data	450	600–900
\dot{E} (erg s ^{−1})	$6 \times 10^{33*}$	5×10^{33}	no data	$1.3 \times 10^{27\#}$	$(2.9–6.6) \times 10^{28\dagger}$
Γ	1.12	2.3	2.14	2.5 (assumed)	2 (assumed)
F_X^\ddagger (erg s ^{−1} cm ^{−2}) .	5.9×10^{-13}	2.8×10^{-13}	1.3×10^{-13}	$< 4.9 \times 10^{-13\S}$	$2.6 (1.0–5.3) \times 10^{-15**}$
L_X (erg s ^{−1}) 	6.0×10^{29}	4.6×10^{29}	9.1×10^{29}	$< 4.3 \times 10^{28\S}$	$5.3 (2.3–10.9) \times 10^{26**}$
$\eta \equiv L_X / \dot{E}$	1.0×10^{-4}	9×10^{-5}	no data	< 33	$0.012 (0.0022–0.074)^{\dagger\dagger}$
References	(1)(2)	(3)(4)(5)	(3)(6)	(7)(8) this work	(3)(9) this work

* Adopted from de Jager (1994) and de Jager et al. (1994).

With the assumption of the radius of 2417 km (see text).

† Estimated with Suto et al. (2023) (see text).

‡ Unabsorbed flux in the 0.5–10 keV band.

§ 3σ upper limit.

|| In the 0.5–10 keV band.

** 90% error range.

†† 90% error range assuming the uncertainty of \dot{E} is also in 90% error range.

Note — (1) Terada et al. (2008), (2) Steinmetz et al. (2020), (3) Gaia Collaboration (2020), (4) Takata et al. (2018), (5) Pelisoli et al. (2022), (6) Schwope et al. (2023), (7) Kawka et al. (2007), (8) Harayama et al. (2013) (9) Caiazzo et al. (2021)

There is some excess emission around the target position. However, it is not significant, and the `wavdetect` command in CIAO did not detect any source in this region. In order to estimate the flux of the possible X-ray emission on this position, we cited the coordinate of the pixel which has the maximum count, (RA, Dec.) = (19:01:32.91, +14:58:09.1). Note that the position is well close to the SIMBAD position as shown in Figure 1. The significance level of this position is estimated with `srcflux` command in CIAO to be 0.998 or 3.5σ level. To convert the count rate to flux, a spectral model is required. We opted for the absorbed power-law model, which is commonly used for both WD pulsars and neutron star pulsars. The absorption column was fixed at 1×10^{20} cm^{−2}, based on the presumption that the interstellar medium density is 1 cm^{−3} and considering a distance of 41 pc (Gaia Collaboration 2020). The photon index of WD pulsars ranges from 1–2.5 (Terada et al. 2008; Takata et al. 2018; Schwope et al. 2023). Based on this, we adopted a value of 2. This value is also typical for neutron star pulsars (Kargaltsev & Pavlov 2008). The resulting unabsorbed flux is $2.4 (0.9–4.8) \times 10^{-15}$ erg s cm^{−2} in the 0.5–7 keV band, where the error range is in 90% confidence level. Adjusting the photon index to 1.5 did not lead to significant changes (only less than a few 10%) in our findings.

4 Discussion

In the previous section, we presented that the strongly magnetized and rapidly rotating WD, ZTF J1901+14, has been detected, although it is not prominently bright in the X-ray band. Assuming a distance of 41 pc, the 90% error range of the 0.5–10 keV luminosity is $5.3 (2.3–10.9) \times 10^{26}$ erg s^{−1}. It is three orders of magnitude lower than the nonthermal X-rays detected from other accreting white dwarf pulsars, which have X-ray luminosities of approximately 10^{29} erg s^{−1} (Terada et al. 2008; Takata et al. 2018; Schwope et al. 2023), as listed in Table 2.

In the case of neutron stars, the spin-down energy \dot{E} and X-ray efficiency η , which is defined as (X-ray luminosity)/ \dot{E} , serve as crucial parameters for their understanding (e.g., Kargaltsev & Pavlov 2008). We thus evaluated \dot{E} and η for our samples and made comparisons. Caiazzo et al. (2021) measured the surface magnetic field B_s and the radius R of ZTF J1901+14 to be between 600–900 MG and 2140_{-230}^{+160} km, respectively. Meanwhile, Suto et al. (2023) proposed that the magnetic field structure of ZTF J1901+14 is dipolar, with the magnetic axis inclined at $\chi=60$ degrees to the rotation axis, based on optical/UV light curve analyses. Assuming the magnetosphere is force free, \dot{E} is estimated to be

$$\dot{E} = \mu^2 \left(\frac{2\pi}{P} \right)^4 c^{-3} (1 + C \sin^2(\chi)) \sim (1.5 - 10) \times 10^{28} \text{ erg s}^{-1}, \quad (1)$$

where $\mu = B_d R^3 / 2$ with the dipole magnetic field B_d , with the assumption of $B_d = B_s$, c is the light speed, and the constant $C \sim 1$ (Gruzinov 2005; Spitkovsky 2006; Tchekhovskoy et al. 2013). For accreting WD pulsars, the \dot{E} of AE Aqr was taken to be 6×10^{33} erg s^{−1}, as estimated by de Jager (1994) and de Jager et al. (1994). For AR Sco, we utilized the

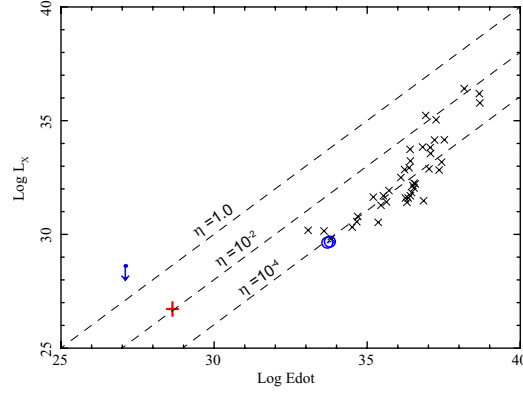


Fig. 2. Spin down energy vs. 0.5–8 keV X-ray luminosity of rotation powered neutron stars (black X; Kargaltsev & Pavlov 2008), accreting WD pulsars AE Aqr and AR Sco (blue circles; Terada et al. 2008; Takata et al. 2018), an isolated WD EUVE J0317–855 (blue upper-limit; Harayama et al. 2013), and ZTF J1901+14 (in red). The upper limits are all in 3σ level, and the error range for ZTF J1901+14 is in 90%. Note that the uncertainty is large with just 3.5σ detection level. The spin-down energy for EUVE J0317–855 is estimated with the WD radius of 2417 km (see table 1. Dashed lines represent η of 1, 1×10^{-2} , and 1×10^{-4} from top to bottom, respectively.

spin-down frequency of $\dot{\nu} = 4.47 \times 10^{-17} \text{ Hz s}^{-1}$ (Pelisoli et al. 2022), resulting in $\dot{E} = 5 \times 10^{33} \text{ erg s}^{-1}$ and $B_d = 900 \text{ MG}$, with assumptions regarding that the spin-down is due to magnetic dipole radiation, $M = 0.8 M_\odot$, and $R = 7000 \text{ km}$. The derived parameters are also listed in Table 2. Regarding X-ray efficiency, η , AE Aqr and AR Sco are approximately 1×10^{-4} , whereas ZTF J1901+14 is 0.012 (0.0022 – 0.074). In contrast, typical neutron stars have η values between 10^{-5} and 10^{-1} (Kargaltsev & Pavlov 2008). We can thus infer that its X-ray efficiency is similar to typical neutron stars, although the uncertainty is rather large. Figure 2 plots the relationship between \dot{E} and X-ray luminosity for our samples compared to neutron stars, further illustrating this point.

We also drew comparisons with another isolated WD pulsar candidate, EUVE J0317–855. Harayama et al. (2013) estimated its $\log \dot{E}$ 29.0–30.8 with the assumption of the radius of 5000–10000 km. On the other hand, the mass of EUVE J0317–855 is $1.31\text{--}1.37 M_\odot$ (Kawka et al. 2007), which is quite similar to that of ZTF J1901+14, and its radius should be as small as that of ZTF J1901+14 according to the mass-radius relation of WDs. We thus re-estimated its $\log \dot{E}$ to be 27.1 (or $\dot{E} = 1.3 \times 10^{27} \text{ erg s}^{-1}$) with the assumed radius of 2417 km (see table 1), following that the magnetic dipole moment $\mu \propto BR^3$ and $\dot{E} \propto \mu^2 P^{-4} \propto B^2 R^6 P^{-4}$. The re-estimated parameters for EUVE J0317–855 are also listed in Table 2. With this \dot{E} , the 3σ upper-limit of the X-ray efficiency for EUVE J0317–855 is 33 in the 0.5–8 keV band, which is much larger the value with larger radius assumptions. Figure 2 also shows the EUVE J0317–855, with the assumptions of our new radius estimation. The figure shows clearly that the X-ray efficiency of ZTF J1901+14 is well constrained compared with that for EUVE J0317–855, although the significance is not so high.

Here, we note the uncertainty of our results. One of the concern is the uncertainty of the derived radius with the model by Nauenberg (1972), which ignored the effect of magnetic field and rotation: the strong magnetic field makes degenerate pressure smaller and the stellar radius becomes larger, and as a result, the derived spin-down energy becomes larger and the X-ray efficiency smaller. This effect clearly appear the magnetic field much larger than $\sim 10^9 \text{ Gauss}$, thus in this sense, our conclusion (not very bright in X-rays) does not change. The error range of the radius for ZTF J1901+14 is just 10% (Caiazzo et al. 2021), which is already included in our discussion. The distance uncertainty is negligible, less than 0.1 pc (Gaia Collaboration 2020).

Assuming that the X-ray detection from ZTF J1901+14 is the case, let us explore the potential emission mechanism. Given the measured radius, magnetic field strength, and rotation period, ZTF J1901+14 is likely below the death line for WD pulsars (Kashiyama et al. 2011), i.e., electron-positron pair multiplication process in the magnetosphere will not be operational. Nevertheless, charged particle could still undergo acceleration through the electric field induced by the unipolar induction, especially along the open field lines. The maximum voltage can be estimated as

$$V_{\text{max}} \approx \frac{B_d (2\pi/P)^2 R^3}{2c^2} \sim 4.2 \times 10^{11} \text{ Volt.} \quad (2)$$

Hereafter, we adopt the maximum values of the radius and magnetic field strength within uncertainties (Caiazzo et al. 2021) as our fiducial values. Accordingly, electrons could be accelerated to sub-TeV energies with Lorentz factors of

$\gamma_{\max} \approx eV_{\max}/m_e c^2 \sim 8.1 \times 10^5$. Assuming that electrons with a Goldreich-Julian density $n_{\text{GJ}} \approx B_d/cP$ are supplied quasi-steadily into the polar cap region $r_{\text{cap}} \approx R \times (2\pi R/cP)^{1/2}$, the kinetic luminosity of the electrons becomes comparable to the spindown luminosity, i.e., $L_e \approx 2\pi r_{\text{cap}}^2 c m_e n_{\text{GJ}} \gamma_{\max} c^2 = 2\mu^2 (2\pi/P)^4 c^{-3} \approx \dot{E}$. These electrons partially lose their energies through the curvature radiation. The emission frequencies can be estimated as

$$h\nu_c \approx \frac{3h\gamma_{\max}^3 c}{4\pi R_c} \sim 69 \text{ keV} \left(\frac{R_c}{R} \right)^{-1} \quad (3)$$

where h is the Planck constant, R_c is the curvature radius of the open field lines. In the case of ZTF 1901+14, the emission is predominantly in the X-ray band for $R \lesssim R_c \lesssim 100R$, i.e., in the near surface region. The X-ray luminosity can be estimated as $L_X \approx (t_c/t_{\text{dyn}}) \times L_e \approx (t_c/t_{\text{dyn}}) \times \dot{E}$, where $t_{\text{dyn}} \approx R/c$ is the dynamical timescale of the electrons and $t_c \approx 3m_e c R_c^2 / 2e^2 \gamma_{\max}^3$ is the energy loss timescale through the curvature radiation. Then, the X-ray radiation efficiency is given as

$$\eta = \frac{L_X}{\dot{E}} \approx \frac{t_{\text{dyn}}}{t_c} \sim 1.3 \times 10^{-3} \left(\frac{R_c}{R} \right)^{-2}. \quad (4)$$

Hence, within the uncertainties, the observed X-ray luminosity of ZTF J1901+14 may be attributed to the curvature radiation from sub-TeV electrons accelerated along the open field lines.

Since $\eta \ll 1$, sub-TeV electrons escape into the interstellar medium without significant energy loss, thus supporting the idea that strongly magnetized, rapidly rotating massive WDs like ZTF J1901+14 are efficient factories for electron cosmic rays (Kashiyama et al. 2011). The lower X-ray efficiency compared to X-ray-bright neutron star pulsars can be attributed to its relatively low-density environment. Relativistic winds and cosmic rays launched from the magnetosphere of ZTF J1901+14 would be directly injected into the interstellar medium, whereas those from a young neutron star pulsar are surrounded by a supernova remnant (e.g., Gelfand et al. 2009; Bamba et al. 2010) and can efficiently dissipate at and beyond the wind termination shock (e.g., Meintjes et al. 2023). Accreting WD pulsars are typically found in environments with a relatively high density of materials from their companion stars, as observed in the case of AE Aqr (Terada et al. 2008), or they may encounter stellar winds from their companion stars, as seen in the case of AR Sco (Buckley et al. 2017; Takata et al. 2018).

Further investigations, such as deeper X-ray observations of ZTF J1901+14 and measurements of the magnetic field of J191213.72–441045.1, will provide more insights into clarifying the differences in non-thermal emissivity among these types of compact star systems. We need deeper X-ray observations with large effective area missions such as Athena (Nandra et al. 2013) and Lynx (Gaskin et al. 2018), in order to make quantitative comparison of X-ray efficiencies of other compact star systems. The requirement of point source sensitivity of Wide Field Imager (WFI) onboard Athena is in the order of $10^{-17} \text{ erg s}^{-1} \text{ cm}^{-2}$ (Nandra et al. 2013), resulting $\eta \sim 10^{-4}$ for ZTF J1901+14, which is enough to judge isolated massive and rapid-rotating WDs are efficient X-ray emitters or not.

5 Summary

We conducted an X-ray search for ZTF J1901+14, one of the most massive and rapidly-rotating white dwarfs, using Chandra and found X-ray emission with the significance of 3.5σ level. Assuming a photon index of 2, we derived its intrinsic flux to be $2.3 (0.9\text{--}4.7) \times 10^{-15} \text{ erg cm}^{-2} \text{ s}^{-1}$ and luminosity $4.6 (2.0\text{--}9.5) \times 10^{26} \text{ erg s}^{-1}$ for a 0.5–7 keV band in the 90% confidence range, given its distance of 41 pc. We derived an X-ray efficiency (η) concerning the spin-down luminosity to be 0.012 (0.0022–0.074), which is similar to typical neutron star pulsars. The observed X-ray emission might suggest that such WDs have the capability to accelerate electrons to sub-TeV energies. However, conclusive evidence requires more in-depth observations. For a comprehensive comparison with other WD pulsars that have companion stars, like AE Aqr, AR Sco, and SDSS J191213.72–441045.1, further X-ray/optical observations are essential to pinpoint physical parameters including the magnetic field and spin-down luminosity.

Acknowledgments

We thank the anonymous referee for his/her constructive comments. We thank Shinpei Shibata for the fruitful discussions. This research has made use of the SIMBAD database, operated at CDS, Strasbourg, France. This work was financially supported by Japan Society for the Promotion of Science Grants-in-Aid for Scientific Research (KAKENHI) Grant Numbers, JP19K03908 (AB), JP23H01211 (AB), JP20K04009 (YT), JP20H01904 (KK), JP22H00130(KK), JP23H04899 (KK), JP21H01078 (SK), JP22H01267

(SK), JP22K03681 (SK), and JP20H00153 (TT).

References

- Bamba, A., Mori, K., & Shibata, S. 2010, *ApJ*, 709, 507
- Bamba, A., Watanabe, E., Mori, K., Shibata, S., Terada, Y., Sano, H., Filipović, M. D. 2020, *Ap&SS*, 365, 178
- Bellm, E. C., et al. 2019, *PASP*, 131, 018002
- Buckley, D. A. H., Meintjes, P. J., Potter, S. B., Marsh, T. R., Gänsicke, B. T. 2017, *Nature Astronomy*, 1, 0029
- Caiazzo, I., et al. 2021, *Nature*, 595, 39
- Dan, M., Rosswog, S., Brüggen, M., Podsiadlowski, P. 2014, *MNRAS*, 438, 14
- Das, U. & Mukhopadhyay, B. 2012, *Phys. Rev. D*, 86, 042001
- de Jager, O. C. 1994, *ApJS*, 90, 775. doi:10.1086/191902
- de Jager, O. C., Meintjes, P. J., O'Donoghue, D., Meintjes, P. J., O'Donoghue, D., Robinson, E. L. 1994, *MNRAS*, 267, 577
- Eisenstein, D. J., et al. 2006, *ApJS*, 167, 40
- Fruscione, A., et al. 2006, *Proc. SPIE*, 6270, 62701V
- Gaia Collaboration 2020, *VizieR Online Data Catalog*, I/350
- García-Berro, E., et al. 2012, *ApJ*, 749, 25
- Gaskin, J. A., et al. 2018, *Proc. SPIE*, 10699, 106990N
- Gelfand, J. D., Slane, P. O., & Zhang, W. 2009, *ApJ*, 703, 2051
- Gruzinov, A. 2005, *Phys. Rev. Lett.*, 94, 021101
- Harayama, A., Terada, Y., Ishida, M., Hayashi, T., Bamba, A., Tashiro, M. S. 2013, *PASJ*, 65, 73
- Hurley-Walker, N., et al. 2022, *Nature*, 601, 526
- Hurley-Walker, N., et al. 2023, *Nature*, 619, 487
- Iwamoto, K., Brachwitz, F., Nomoto, K., Kishimoto, N., Umeda, H., Raphael Hix, W., Thielemann, K. 1999, *ApJS*, 125, 439
- Kamae, T., Lee, S.-H., Makishima, K., Shibata, S., Shigeyama, T. 2018, *PASJ*, 70, 29
- Kargaltsev, O. & Pavlov, G. G. 2008, *40 Years of Pulsars: Millisecond Pulsars, Magnetars and More*, 983, 171
- Kashiyama, K., Ioka, K., & Kawanaka, N. 2011, *Phys. Rev. D*, 83, 023002
- Kawka, A., Vennes, S., Schmidt, G. D., Wickramasinghe, D. T., Koch, R. 2007, *ApJ*, 654, 499
- Kilic, M., Kosakowski, A., Moss, A. G., Bergeron, P., Conly, A. A. 2021, *ApJL*, 923, L6
- Kilic, M., et al. 2023, *MNRAS*, 518, 2341
- Kisaka, S. & Tanaka, S. J. 2017, *ApJ*, 837, 76
- Marsh, T. R., et al. 2016, *Nature*, 537, 374
- Meintjes, P. J., Madzime, S. T., Kaplan, Q., van Heerden, H. J. 2023, *Galaxies*, 11, 14
- Nandra, K., et al. 2013, *arXiv:1306.2307*
- Nauenberg, M. 1972, *ApJ*, 175, 417
- Ostriker, J. P., Rees, M. J., & Silk, J. 1970, *Astrophys. Lett.*, 6, 179
- Pelisoli, I., et al. 2022, *MNRAS*, 516, 5052
- Pelisoli, I., et al. 2023, *Nature Astronomy*, 2023, 7, 931
- Schwab, J. 2021, *ApJ*, 906, 53
- Schwope, A., Marsh, T. R., Standke, A., Pelisoli, I., Potter, S., Buckley, D., Munday, J., Dhillon, V. 2023, *A&A*, 674, L9
- Seitenzahl, I. R., et al. 2013, *MNRAS*, 429, 1156
- Shibata, S., Watanabe, E., Yatsu, Y., Enoto, T., Bamba, A. 2016, *ApJ*, 833, 59
- Spitkovsky, A. 2006, *ApJL*, 648, L51
- Steinmetz, M., et al. 2020, *AJ*, 160, 83
- Suto, Y., Sasaki, S., Aizawa, M., Fujisawa, K., Kashiyama, K. 2023, *PASJ*, 75, 103.
- Takata, J., Hu, C.-P., Lin, L. C. C., Tam, P. H. T., Pal, P. S., Hui, C. Y., Kong, A. K. H., Cheng, K. S. 2018, *ApJ*, 853, 106
- Tchekhovskoy, A., Spitkovsky, A., & Li, J. G. 2013, *MNRAS*, 435, L1
- Terada, Y., et al. 2008, *PASJ*, 60, 387
- Tout, C. A., Wickramasinghe, D. T., Liebert, J., Ferrario, L., Pringle, J. E. 2008, *MNRAS*, 387, 897
- Watanabe, E., Shibata, S., Sakamoto, T., Bamba, A. 2019, *MNRAS*, 486, 5323
- Weisskopf, M. C., Brinkman, B., Canizares, C., Garmire, G., Murray, S., Van Speybroeck, L. P. 2002, *PASP*, 114, 1
- Wenger, M., et al. 2000, *A&AS*, 143, 9